BHM (2012) Vol. 157 (8–9): 301–305
DOI 10.1007/s00501-012-0034-7

BHM Berg- und Hüttenmännische Monatshefte

Phase Selection in 6082 Al-Mg-Si Alloys

Alexander Wimmer[1,2], Jiehua Lee[3] and Peter Schumacher[3,4]

[1]Kompetenzzentrum Automobil- und Industrie-Elektronik GmbH, Villach, Austria
[2]Erich Schmid Institute of Materials Science, Austrian Academy of Sciences, Leoben, Austria
[3]Chair of Casting Research, Department of Metallurgy, Montanuniversitaet Leoben, Leoben, Austria
[4]Österreichisches Gießerei-Institut, Leoben, Austria

Received June 15, 2012; accepted June 27, 2012; published online September 18, 2012

Abstract: In this work two new kinds of particles in continuous casted 6082 alloy were observed. nm-size Al(Fe,Mn,Cr)Si particles and large U2-AlMgSi particles were found secondary to the expected, coarse Al(Fe,Mn,Cr)Si and Mg_2Si on the grain boundaries and nm-size Mg_2Si inside the grains. Because of the small size of the Al(Fe,Mn,Cr)Si precipitations an increase of the strength of the alloy is expected.

Keywords: 6082, Aluminium, Mg_2Si, AlFeSi, U2-AlMgSi

Ausscheidungen in 6082 Al-Mg-Si Legierungen

Zusammenfassung: In der vorliegenden Arbeit wurden zwei, bisher nicht beschriebene Ausscheidungen in einer 6082 Al-Mg-Si Legierung gefunden. Es wurden nm-große Al(Fe,Mn,Cr)Si Ausscheidungen sowie µm-große U2-AlMgSi Ausscheidungen neben den erwarteten, groben Al(Fe,Mn,Cr)Si und Mg_2Si Teilchen an den Korngrenzen und nm-großen Mg_2Si Ausscheidungen in den Körnern gefunden. Aufgrund der Größe der Al(Fe,Mn,Cr)Si Teilchen im nm-Bereich ist eine Festigkeitssteigerung durch diese Teilchen zu erwarten.

Schlüsselwörter: 6082, Aluminium, Mg_2Si, AlFeSi, U2-AlMgSi

1. Introduction

Aluminum and especially 6082 Al-Mg-Si alloys are widely used because of their low density and high, tunable strength. Besides heat treatment the microstructure especially influences the properties of the material. Up to now two different kinds of phases were reported.

First the strength increasing Mg/Si phases.

A. Wimmer (✉)
Kompetenzzentrum Automobil- und Industrie-Elektronik GmbH, Villach, Austria
e-mail: alexander.wimmer@k-ai.at

Both Mg and Si are soluble at higher temperatures in solid (and liquid) aluminium, but during cooling they precipitate dependent on the cooling conditions in a different type of morphology (Table 1) [2, 5].

Up to now only β and Si have been reported as coarse (>1 µm) particles, all other particles in Table 1 have been reported as nm-size (<<1 µm) particles.

Secondly there are Al(Fe, Mn,Cr)Si phases in Al-Mg-Si alloys (6xxx), especially in 6082 alloy. AlFeSi is the common name of iron-containing phases, however the correct composition is Al(Fe, Mn,Cr)Si, because this phase also contains a significant amount of Mn and Cr in case of the alloy 6082.

There are different structures of AlFeSi intermetallics (Table 2) [7].

During casting, Fe precipitates mainly as AlFeSi on the grain boundaries [3].

There are three different crystal structures associated with morphologies of AlFeSi:

monoclinic β-AlFeSi	a = b = 0.612 nm, c = 4.15 nm, β = 91°
cubic α-AlFeSi	a = 1.252–1.256 nm
hexagonal α'-AlFeSi	a = 1.23 nm, c = 2.62 nm

In the as cast billets most of AlFeSi exist as platelets with a monoclinic β-AlFeSi crystal structure on the grain boundaries [1], the particles have a length of ~10 µm, the thickness is in the range of 100 nm[4]. This β-AlFeSi causes deformation cracks during billet extrusion because of the small cohesion between the precipitations and the Al matrix (pick-up effect [6]). Furthermore, the monoclinic phase is very brittle, which contributes to crack formation [1]. A further reason for cracks caused by the β-phase is a stress field around the precipitations due to volume changes during precipitation [6].

During heat treatment the platelets of β-AlFeSi transform into pearl necklace distributed α-AlFeSi [1]. The transformation starts on the surface of the β platelets, the driving force for the transformation is the smaller surface

TABLE 1:
Different types of Mg/Si precipitations [8]. The table shows the different kinds of particles which could appear in 6xxx alloys. The shape describes the morphology, the formula the chemical composition. a, b and c describe the lattice dimensions, β and γ the angles of the lattice

Phase	Shape	Formula	Space group	a (nm)	b (nm)	c (nm)	β	γ
GP-zone	Needle	$AlMg_4Si_6$	C2/m	1.48	0.405	0.648	105.3°	
GP-zone	Plate	Si/Mg = 1	(fcc $L1_0$)	0.405				
β''	Needle	Mg_5Si_6	C2/m	1.516	0.405	0.674	105.3°	
β''	Needle	$Mg_{1.8}Si$	$P6_3$	0.715	0.715	0.405		120°
B' (C)	Lath	Mg/Si~1	Hexagonal	1.04		0.405		120°
U1 (A)	Needle	$MgAl_2Si_2$	P_{-3m1}	0.405		0.674		120°
U2 (B)	Needle	AlMgSi	Pnma	0.675	0.405	0.794		
β	Plate/cube	Mg_2Si	F_{m-3m}	0.6354				
Si	Plate	Si	F_{d3m}	0.5431				

TABLE 2:
Different types of AlFeSi [7]. The composition describes the chemical structure of the alloy, the Fe:Si ratio the ratio between iron and silicon and is important for diversification of the different kinds of AlFeSi

Intermetallic phase	Composition	Fe:Si ratio
α-AlFeSi	Al_7Fe_3Si	6
	$Al_{12}Fe_3Si$	6
	Al_8Fe_2Si	4
	$Al_{15}Fe_3Si_2$	3
β-AlFeSi	Al_5FeSi	2
π-AlFeSiMg	$Al_8FeMg_3Si_6$	1/6

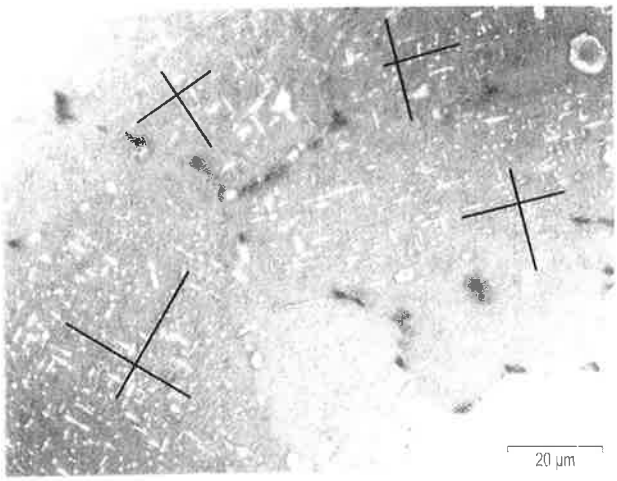

Fig. 1: Etching pits in LOM, 1,000x. White lines in the picture are etching pits, caused by chemical etching of the nm-size precipitations in the grains. The black crosses display the orientation of the coherent particles and as a result the orientation of the grains

energy of the α [1, 6]. The reaction is diffusion controlled and responds to the Johnson-Mehl-Avrami equation [1]. The diffusion of Fe is much slower than the diffusion of Si, as a result the speed of Fe diffusion limits the transformation speed [1].

During the β to α transformation, the Si content of the AlFeSi decreases and the Fe content increases, because Fe from the matrix (and also from other precipitations) diffuses into the AlFeSi particles. Al_3Fe, $AlFeSi_2$ and Al_3FeSi cannot exist in 6082 alloy as the small Fe content does not permit their formation under the given process conditions [1].

2. Methods

For observation of the particles LOM (AXIO Imager A1, Zeiss), SEM (Quanta 200 3d, FEI, operating at 20 kV), EDX (INCA, Energy 200, Oxford Instruments) and TEM (Philips CM12, operating at 120 kV) were used. For the SEM, polished samples were used. The accuracy of the EDX result is ±0.1 % because of fluorescence, absorption and influences of the atomic number. For TEM samples the material was ground, polished and dimpled to a thickness of 30 µm and finally ion polished (Precision Ion Polishing System PIPS, Gatan model 691).

For Barker etching a mixture of 13 g boric acid, 35 g HF, 800 ml H_2O at a voltage of 20 V for 45 seconds was used.

3. Results

Through Barker etching, etching pits of coherent, the strength increasing sub-µm size Mg_2Si phases were observed (Fig. 1), these particles were also observed in Fig. 2. This is an easy method to observe strength increasing particles without costly preparation of TEM samples.

In Figs. 3 and 4a Mg/Si phase with a very low Mg:Si ratio (~1, Table 3) was observed instead of the expected Mg_2Si. As the Mg:Si ratio is smaller than 1, it is impossible that the phase is consistent with Mg_2Si, because for Mg_2Si the Mg:Si ratio is 1.73–2.20.

In literature [7] an $Al_8FeMg_3Si_6$ phase is reported, Thermo-Calc recognizes also the existence of $Al_8FeMg_3Si_6$, but

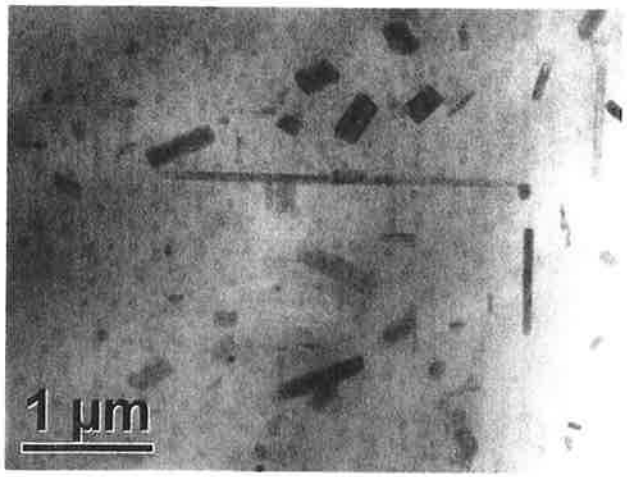

Fig. 2: Coherent particles in TEM, 20,000x. The coherent nm-size precipitations of Mg/Si are coherent with the lattice

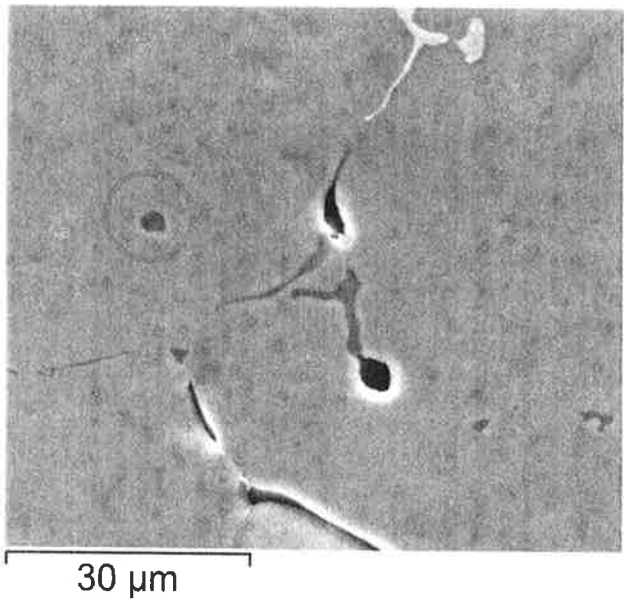

Fig. 3: AlMgSi particle inside a grain. Furthermore AlFeSi (*white*) and Mg/Si (*grey*) on the grain boundary are visible, holes are caused by the etching process

TABLE 3:
Composition of a typical AlMgSi particle. The chemical composition of the particles in atomic percent is shown, results were obtained with EDX

Element atom(%)	Aluminium Al	Silicon Si	Magnesium Mg
EDX	35.1	30.0	34.9

the observed Mg/Si phase does not contain Fe. Because of the Al:Mg:Si ratio of ~1:1:1 this phase is most probably U2-AlMgSi, which was reported up to now only as a coherent nm-size phase.

The most outstanding phase which was observed in this work is nm-sized Al(Fe,Mn,Cr)Si.

Normally the Mn:Fe ratio in coarse Al(Fe,Mn,Cr)Si on the grain boundary is 0.9 [9]. In the observed small Al(Fe,Mn,Cr)Si particles inside the grain (Figs. 5, 6 and 7) the Mn:Fe ratio is >>1 which could be seen in Fig. 5b, sometimes with undetectable amount of Fe, as a result this particles are more correctly AlMnSi particles. Because of the size in the range of ~100 nm this particles could affect the strength of the alloy in a positive manner (the hardness affecting, intermetallic phase θ"-Al_2Cu is also about 100 nm in size and is an important particle in 2xxx Al-Cu alloys).

Up to now the Fe-phases were undesirable in 6xxx alloys, but through these observations the negative Fe-phase could also have a positive side.

4. Discussion

In this work an easy LOM method was found to observe particles which could normally only be seen in the TEM. Through this the existence of essential strength-increasing particles can be proofed.

Furthermore two new particle types were observed: An U2-AlMgSi phase, which is normally in the range of 10 nm (Fig. 8a), was observed with a size >1 µm (Fig. 8b). On the other hand, Al(Fe,Mn,Cr)Si precipitations were found inside the grain with a size <100 nm (Fig. 8c), normally

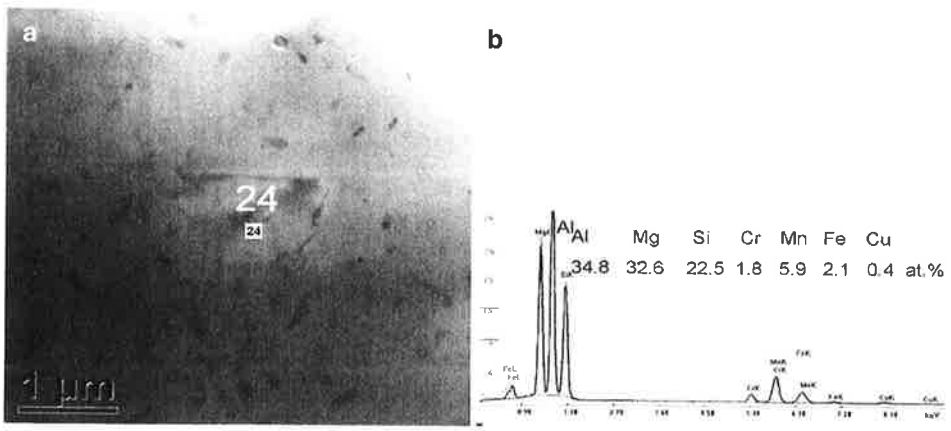

Fig. 4: (a) AlMgSi particle, (b) EDX result. Beyond the expected nm-size Mg/Si phases also a µm-size AlMgSi particle was detected with TEM. The EDX analysis and diffraction pattern verified that this particle is U2-AlMgSi

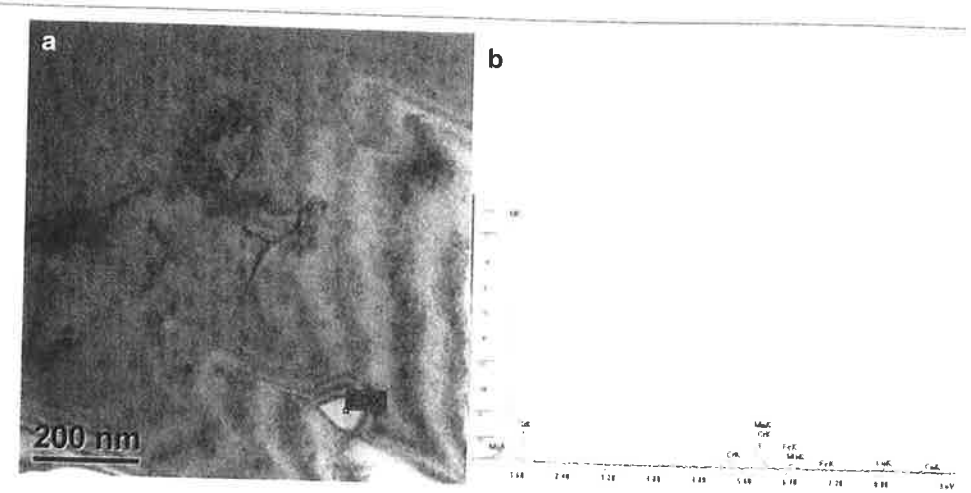

Fig. 5: (a) Mn rich AlMnSi particle, size ~100 nm, (b) EDX-result. The picture shows an AlMnSi particle (*grey*), furthermore fringes which are artefacts from sample preparation

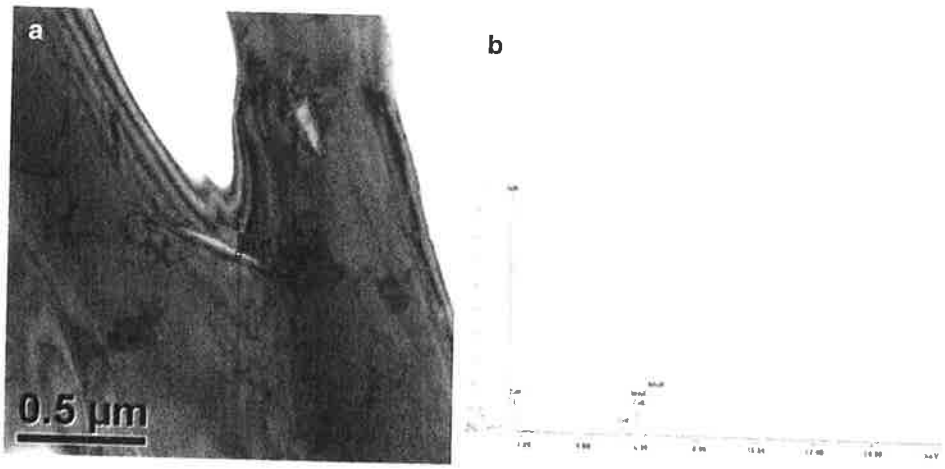

Fig. 6: (a) Mn rich AlMnSi particle, size ~400 x 50 nm, (b) EDX-result. A plate shaped AlMnSi particle is shown in grey, in the white areas there is a hole in the sample

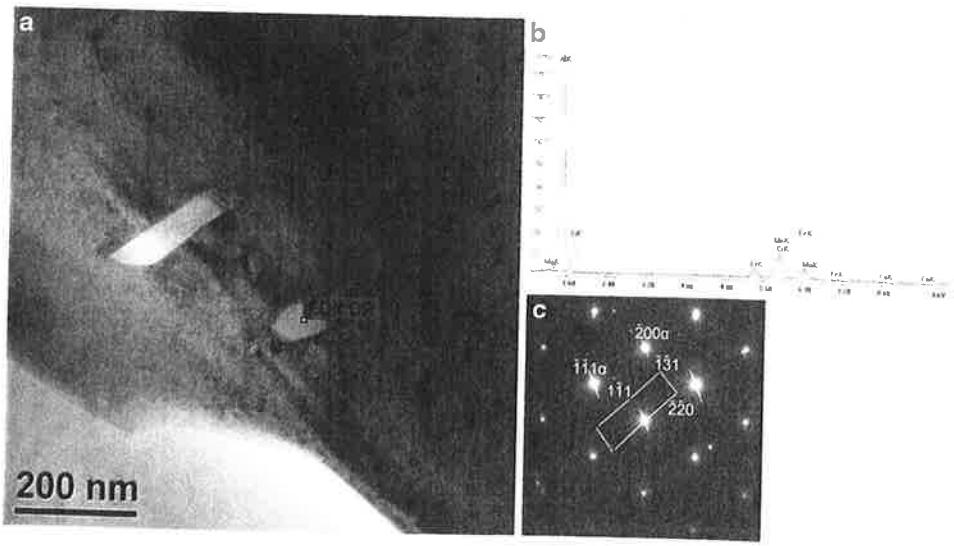

Fig. 7: (a) Mn rich AlMnSi particle, size ~100 nm, (b) EDX-result, (c) Diffraction pattern. The rounded, grey particle consists mainly of Al, Mn and Si, the diffraction pattern verifies that this particle is an α-AlMnSi precipitation

Al(Fe,Mn,Cr)Si only exists on the grain boundary as a >1 µm phase (Fig. 8d).

This work shows that the microstructure of the common metal aluminum and its alloys is not clarified 100% up to now and there are still some further starting points to optimize the properties of 6xxx alloys.

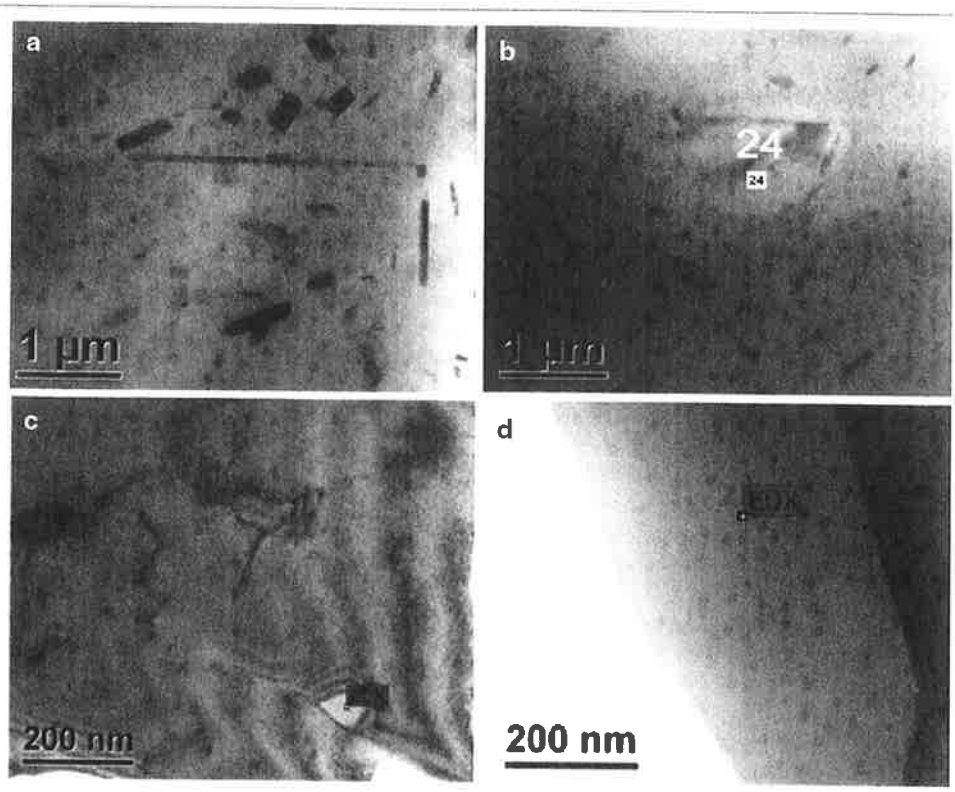

Fig. 8: Precipitations in 6082 alloy. **a** nm-size Mg/Si particles. **b** µm-size U2-AlMgSi particle. **c** nm-size Al(Fe, Mn,Cr)Si particles. **d** µm-size Al(Fe, Mn,Cr)Si particles .This Figure with TEM images compares the expected particles (**a** and **d**) with the unexpected particles (**b** and **c**)

References

1. N. C. W. Kuijpers, F. J. Vermolen, C. Vuik, P. T. G. Koenis, K. E. Nilsen, S. Van Der Zwaag, The dependence of the β-AlFeSi to α-Al(Fe, Mn) Si transformation kinetics in Al–Mg–Si alloys on the alloying elements, Materials Science and Engineering A, Volume 394, Issues 1–2, 15 March (2005), pp. 9–19
2. G. Mrówka-Nowotnik, J. Sieniawski, Influence of heat treatment on the microstructure and mechanical properties of 6005 and 6082 aluminium alloys, Journal of Material Processing Technology, Volume 162–163, (2005), pp. 367–372
3. H. Tanihata, T. Sugawara, K. Matsuda, S. Ikeno, Effect of casting and homogenizing treatment conditions on the formation of Al–Fe–Si intermetallic compounds in 6063 Al–Mg–Si alloys, Journal of Materials Science, Volume 34, Number 6, (1999), pp. 1205–1210
4. N. C. W. Kuijpers, W. H. Kool, P. T. G. Koenis, K. E. Nilsen, I. Todd, S. Van Der Zwaag, Assessment of different techniques for quantification of α-Al(Fe, Mn)Si and β-AlFeSi intermetallics in AA 6xxx alloys, Volume 49, Issue 5, December (2002), pp. 409–420
5. J. L. Cavazos, R. Colás, Precipitation in a heat-treatable aluminium alloy cooled at different rates, Materials Characterization, Volume 47, Issues 3–4, September-October (2001), pp. 175–179
6. S. R. Claves, D. L. Elias, W. Z. Misiolek, Analysis of the intermetallic phase transformation occurring during homogenization of 6xxx aluminum alloys, Materials Science Forum, Volumes 396–402, Part 2, (2002), pp. 667–674.
7. M. A. Cooksey, N. Danilova, B. Rinderer, M. J. Couper, Process performance of continuous billet homogenisers, 6th Australian Asian Pacific Conference on Aluminium Cast House Technology, The Minerals, Metals and Materials Society, (1999), pp. 309–318
8. S. Camero, E. S. Puchi, G. Gonzalez, Effect of 0.1% vanadium addition on precipitation behaviour and mechanical properties of Al-6063 commercial alloy, J Mater Sci, Volume 41, (2006), pp. 7361–7373
9. A. Wimmer, Influence of the homogenization treatment on the precipitation and dissolution of intermetallic phases and effects on extrudability in direct chilled Al-Mg-Si alloys, Master thesis, University of Leoben, (2011), pp. 62–63